CHAPTER VI
EFFECTUAL DRUG-RELEASING POROUS SCAFFOLDS FROM 1,6-DIISOCYANATOHEXANE-EXTENDED POLY(1,4-BUTYLENE SUCCINATE) FOR BONE TISSUE REGENERATION

6.1 Abstract

Tooth extraction induces residual ridge resorption which impairs function and aesthetic of dental prostheses. This study aimed at developing new bone scaffolds to be used in a tooth socket for preserving bone mass from the residual ridge resorption. Scaffolds were fabricated from poly(1,4-butylene succinate) extended with 1,6-diisocyanatohexane (PBSu-DCH) by solvent casting and particulate leaching technique. Four different weight ratios of NaCl particles (200-400 μm; used as the porogen species) and the polymer were varied (i.e., 25, 30, 35, and 40% based on the weight of the polymer). Scaffolds were evaluated for their physical (i.e., morphology, porosity, pore volume, and pore size), physico-mechanical (i.e., mechanical properties and water absorption capability), and biological properties (i.e., cytotoxicity and bone cell attachment). The potential for use of the as-prepared materials as effectual drug-releasing scaffolds for bone tissue regeneration was assessed by incorporating ipriflavone and studying the release of the drug from the drug-loaded scaffolds.

(**Key-words**: bone scaffolds; particulate leaching; poly(butylene succinate)

6.2 Introduction

"Residual ridge" is a term used in dentistry to describe the shape of the clinical alveolar ridge existing after a complete healing of bone and soft tissues once a tooth had been extracted (Bodic *et al.*, 2005). Improper shape or size of the residual ridge due to severe bone resorption diminishes dental prosthetic replacement to achieve aesthetic and function. Factually, resorption of the residual ridge is a chronically irreversible and cumulative mechanism (Jahangiri *et al.*, 1998). It occurs

continuously within the first year, with a particularly fast rate during the first 3 to 6 months (Jahangiri *et al.*, 1998; Bodic *et al.*, 2005). The resorption continues at a slower pace throughout a life-span, resulting in the removal of a large amount of jaw bone. It was estimated that bone loss occurred at ~21, ~36, and ~44% after a tooth had been extracted for 3, 6, and 12 months, respectively, and the alveolar bone may lose up to 10 mm of the lower jaw height after 25 years (Bodic *et al.*, 2005). Prevention of the alveolar bone resorption caused by a tooth extraction, therefore, has been of great concern.

To preserve bone mass, various materials, e.g., autogenous or allogenic bone grafts (Wiesen and Krrzis, 1998), hydroxyapatite-collagen implant materials (Hanne *et al.*, 1998), and chemical agents like bisphosphonates (Yaffe *et al.*, 1999; Altundal and Guvener, 2004), have been administered into the dental socket immediately after a tooth extraction. In the tissue engineering point of view, development of three-dimensional scaffolding biomaterials is a means for filling bone lesions (Hutmacher, 2000). Apart from the general characteristics of an ideal bone scaffold, a suitable scaffold for the dental socket should be soft, but strong enough to be easily placed in site without rupture or shape relapse. Synthetic biodegradable polyester is a material of choice due to its several promising properties. The gradual resorption behavior of this type of material is conducive to being concomitantly substituted with new bone mass (Drotleff *et al.*, 2004). Such a material can be tailored by a variety of fabrication methods to achieve the desired internal architecture that allows bone cells to move in and supports their attachment to the construct simultaneously (Griffith, 2000; Wiesmann *et al.*, 2004).

Poly(1,4-butylene succinate) (PBSu) is an aliphatic biodegradable thermoplastic polyester, synthesized through a condensation polymerization of succinic acid and 1,4-butane diol. PBSu was proven to be biocompatible with osteoblasts, due to its ability in supporting both the proliferation and the differentiation of the cells (Li *et al.*, 2005). However, with a melting temperature (T_m) in the range of 90-120°C, PBS with a low T_m is anticipated to possess an improved biodegradability. This could be achieved by an introduction of a certain type of non-crystallizable units into the polymer chains, which causes both the T_m and the crystallinity to decrease, when compared with those of the pure polymer

(Nikolic *et al.*, 2003). 1,6-diisocyanatohexane-extended PBSu (hereafter, PBSu-DCH) is one such modification that was developed by coupling PBSu with hexamethylene diisocyanate as a chain extender (Nikolic and Djonlagic, 2001). In the tissue engineering point of view, the properties of PBSu-DCH are expected to be improved over those of the pure PBS and it is of our great interest to investigate whether PBSu-DCH is a suitable material for the preparation of scaffolds that enhance the regeneration of bone in the dental socket.

The present contribution focused on the fabrication of porous PBSu-DCH scaffolds by solvent casting and particulate leaching technique and the characterization of their properties pertinent to bone tissue regeneration. The effect of porogen/polymer weight ratio on architecture and characteristics of the as-prepared scaffolds was investigated. The potential for use of these scaffolds as carriers for delivery of an active substance suitable for enhancing bone tissue regeneration was investigated using ipriflavone (see Figure 6.8 in Supporting Information for chemical structure), a synthetic derivative of isoflavone which has been known to accelerate osteoblast cell activity and, at the same time, inhibits bone resorption (Civitelli, 1997), as the model compound.

6.3 Experimental

6.3.1 Materials

Poly(1,4-butylene succinate) extended with 1,6-diisocyanatohexane (PBSu-DCH; pellet form; MW 06242; Batch #09717) and 7-(1-methylethoxy)-3-phenyl-4H-1-benzopyran-4-one or 7-isopropoxyisoflavone (hereafter, ipriflavone; 97% purity) were purchased from Aldrich (USA). Chloroform (analytical reagent grade) was purchased from Labscan (Asia) (Thailand). Sodium chloride (NaCl; powder form) was purchased from Ajax Finechem (Australia). All other reagents were of analytical reagent grade and used without further purification.

6.3.2 Preparation of neat and ipriflavone-loaded PBSu-DCH scaffolds

Both the neat and the ipriflavone-loaded PBSu-DCH scaffolds were fabricated by the solvent casting and particulate leaching technique. First, PBSu-DCH pellets were dissolved in chloroform at 50°C to obtain the PBSu-DCH solution

at a fixed concentration of 15% w/v. The solution was left to cool down to room temperature. For the preparation of the drug-loaded scaffolds, ipriflavone (10% based on the weight of the polymer) was dissolved in the PBSu-DCH solution at this stage. NaCl particles, *a priori* sieved to obtain particles with diameters in the range of 200-400 μm, were then added into the neat or the drug-loaded solutions at 4 different NaCl to PBSu-DCH weight ratios (i.e., 25, 30, 35, and 40% w/w). The pasty suspensions were homogenized and a volume of the suspensions was filled with slight pressing in home-made cylindrical glass molds and Petri dishes to obtain molding samples of two different shapes and dimensions. The moldings were placed in a fume hood overnight to allow evaporation of the solvent. NaCl particles were then leached out by immersing the moldings in deionized (DI) water for 48 h, with DI water being replaced every 8 h. The obtained scaffolds were dried *in vacuo* at room temperature for 24 h. Hereafter, the scaffolds that were prepared with the NaCl to PBSu-DCH weight ratios of 25, 30, 35, and 40% w/w were denoted 25x, 30x, 35x, and 40xNaCl scaffolds, respectively. The dimension of the scaffolds obtained from the moldings cast in the home-made cylindrical glass molds (hereafter, cylindrical scaffolds) was 11.3 ± 0.2 mm in diameter and 8.6 ± 0.3 mm in height, while the moldings cast in the Petri dishes were later cut into a desired shape and size for further uses.

6.3.3 Characterization

6.3.3.1 Microstructure observation

One cylindrical scaffold was randomly selected from each group of samples. It was cut into pieces along both the longitudinal and the transverse directions. The cut pieces were mounted on copper stubs, coated with gold using a JEOL JFC-1100 sputtering device, and observed for their microscopic structure using JEOL JSM-5200 scanning electron microscopy (SEM).

6.3.3.2 Porosity, pore volume, and pore size

Porosity and pore volume of the scaffolds were measured gravimetrically according to the following equations:

$$\text{Porosity (\%)} = (1 - \rho_{scaffold}/\rho_{polymer}) \times 100, \quad (1)$$

$$\text{Pore volume (\%)} = (1/\rho scaffold - 1/\rho polymer) \times 100. \quad (2)$$

where $\rho_{polymer}$ is the density of the polymer from which the scaffolds were fabricated and $\rho_{scaffold}$ is the apparent density of the scaffolds which was measured by a Sartorius YDK01 density measurement kit. Here, $\rho_{PBSu\text{-}DCH}$ was taken the value of 1.2 g·cm^{-3}. Five specimens were measured for both the porosity and the pore volume and an average value for each property was calculated. On the other hand, pore size of the scaffolds was directly measured from SEM images, using a UTHSCSA Image Tool version 3.0 software. At least 25 pores for each of the cross and the longitudinal sections (i.e., at least 50 pores in total) were measured and the average values for all of the scaffolds investigated were calculated.

6.3.3.3 Mechanical properties

Both tensile and compressive properties of the scaffolds were determined in their dry state with a Lloyd LRX universal testing machine using 500 N load cell at room temperature. For the tensile test, specimens (50 × 15 × 3 mm^3) were cut from the moldings that had been cast in the Petri dishes. The gauge length was 30 mm and the crosshead speed was 5 mm·min^{-1}. For the compressive test, the cylindrical scaffolds were compressed at the crosshead speed of 1 mm·min^{-1} until the specimens were ~70% deformed from their original height of ~8.6 mm. The tensile test was carried out in pentuplicate and the compressive test was in triplicate.

6.3.3.4 Water absorption capability

The scaffold specimens, cut from the moldings that had been cast in the Petri dishes (circular shape with 15 mm in diameter and 3 mm in height), were first dried, weighed, and individually immersed in 10 mL of 10 mM phosphate buffer saline solution (PBS; pH 7.4) at room temperature. At a given time point, the specimens were taken out, blotted on a glass plate which was set at ~30° from a horizontal baseline for 5 s to remove excess water, and immediately weighed. The amount of water absorbed in the specimens was determined according to the following equation:

$$\text{Water absorption (\%)} = [(W_w - W_d)/W_w] \times 100, \qquad (3)$$

where W_d and W_w are the weight of the specimens before and after submersion in the medium, respectively. The experiment was carried out in pentuplicate and the measurements were carried out at different time intervals within a period of 30 d.

6.3.3.5 In vitro degradation

The cylindrical scaffolds were individually placed in 15 mL of PBS and conditioned at 37°C in a water bath without shaking. The PBS medium was refreshed once a week to maintain the buffer capacity of the medium. At a given time point, the scaffolds were removed, washed twice with DI water, and dried *in vacuo* for 24 h. The remaining weight of the scaffolds was determined as the weight ratio based on the initial weight of the scaffolds, according to the following equation:

$$\text{Remaining weight (\%)} = W_t/W_0 \times 100, \quad (4)$$

where W_0 is the initial weight of the scaffolds in their dry state and W_t is the weight of the scaffolds after the degradation assay in their dry state. The experiment was carried out in triplicate. Any change in the microstructure of the scaffolds after the degradation assay was observed by SEM.

6.3.3.6 Cytotoxicity and cell/scaffold interaction

Mouse calvaria-derived, pre-osteoblastic cells (MC3T3-E1; ATCC CRL-2593) were cultured as a monolayer in minimum essential medium (MEM; Sigma-Aldrich, USA), supplemented by 10% fetal bovine serum (FBS; Biochrom, Germany), 1% L-glutamine (Invitrogen, USA) and a 1% antibiotic and antimycotic formulation [containing penicillin G sodium, streptomycin sulfate, and amphopericin B (Invitrogen Corp.)]. The cells were maintained at 37°C in a humidified atmosphere containing 5% CO_2 and passaged once every 3-4 d.

Only the 35xNaCl scaffolds were used in these studies. Cytotoxicity of the as-prepared scaffolds was evaluated by the indirect cytotoxicity method, using MC3T3-E1 as the reference cells. First, the extraction media were prepared by immersing the scaffold specimens, cut from the moldings that had been cast in the Petri dishes (circular shape with 15 mm in diameter and 3 mm in height), in 500 μL of serum-free medium (SFM; containing MEM, 1% L-glutamine, 1% lactabumin, and 1% antibiotic and antimycotic formulation) for 24 h. Each of these extraction media was used in the indirect cytotoxicity evaluation. MC3T3-E1 were cultured in wells of a 24-well culture plate at 3×10^4 cells/well in serum-containing MEM for 16 h to allow cell attachment on the plate. The cells were then starved with SFM for 24 h, after which time the medium was replaced with an extraction medium. After 24 h of cell culturing in the extraction medium, a 3-(4,5-dimethylthiazol-2-yl)-

2,5-diphenyl-tetrazolium bromide (MTT) assay was carried out to determine the viability of the cells. The experiment was carried out in quadruplicate.

The MTT assay is based on the reduction of the yellow tetrazolium salt to purple formazan crystals by dehydrogenase enzymes secreted from the mitochondria of metabolically active cells. The amount of purple formazan crystals formed is proportional to the number of viable cells. First, each culture medium was aspirated and replaced with 500 μL/well of MTT solution at 0.5 $mg \cdot mL^{-1}$ for a 24-well culture plate. Secondly, the plate was incubated for 1 h at 37°C. The solution was then aspirated and 1 mL/well of dimethylsulfoxide (DMSO) containing 125 μL/well of glycine buffer (pH 10) was added to dissolve the formazan crystals. Finally, after 5 min of rotary agitation, the absorbance of the DMSO solution at 540 nm was measured using a Thermospectronic Genesis10 UV/Visible spectrophotometer.

A primary evaluation for the cell/scaffold interaction was carried out by a direct morphological observation of MC3T3-E1 that were seeded on the surface of the scaffold specimens. Specifically, the scaffold specimens, cut from the moldings that had been cast in the Petri dishes (circular shape with 15 mm in diameter and 3 mm in height), were put in wells of a 24-well culture plate and sterilized with 1 mL of 70% ethanol for 30 min. They were then washed with sterilized DI water twice and later immersed in MEM overnight. MC3T3-E1 were then seeded on the surfaces of the specimens at 3×10^4 cells/specimen in a minimum volume of the culture medium and were allowed to attach on the surfaces for 3 h prior to the addition of 1.5 mL/well of the culture medium. The cells were cultivated at 37°C in a humidified atmosphere containing 5% CO_2 for 24 h, after which time morphology of the attached cells was observed by SEM. After removal of the culture medium, the cell-cultured scaffold specimens were rinsed with PBS twice and the cells were then fixed with 3% gluteraldehyde solution, which was diluted from 50% glutaraldehyde solution (Electron Microscopy Science, USA) with PBS for 30 min. The specimens were then dehydrated in ethanol solutions of varying concentration (i.e., 30, 50, 70, 90, and 100%, respectively) for ~2 min at each concentration, further dried in 100% hexamethyldisilazane (HMDS; Sigma, USA) for 5 min, and later dried

in air after the removal of HMDS. Finally, the specimens were mounted on SEM stubs, coated with gold, and observed by SEM. The examinations were performed on 3 randomly-selected scaffold specimens.

6.3.3.7 Inclusion, content, and release of ipriflavone

A Thermo Nicolet Nexus® 670 Fourier-transformed infrared spectrophotometer (FT-IR) was used to obtain the FT-IR spectra using the KBr disk method in order to confirm the existence of ipriflavone in the drug-loaded scaffolds, while a Shimadzu 2550 UV-Vis spectrophotometer (UV-Vis) was used to determine the amount of the drug loaded in the scaffolds against a predetermined calibration curve for ipriflavone (see Figure 6.9 in Supporting Information). In the latter, the drug-loaded scaffold specimens were completely dissolved in chloroform and the amount of the as-loaded ipriflavone was measured in triplicate at the maximum wavelength of 249 nm. In the drug release assay, the drug-loaded scaffold specimens, cut from the moldings that had been cast in the Petri dishes (circular shape with 15 mm in diameter and 3 mm in height), were immersed in 10 mL of PBS containing 0.15% w/v sodium dodecyl sulfate (SDS) (Perugini *et al.*, 2003) and incubated in a shaking water bath (50 rpm) at 37°C. At a given time point, an amount of the buffer solution (hereafter, the sample solution) was taken out and an equal amount of fresh medium was added in order to maintain a constant volume of the medium. The amount of the drug in the sample solution was determined spectrophotometrically at 249 nm. The experiment was carried out in triplicate.

6.3.4 Statistical analysis

Data were analyzed using the SPSS software version 14.0 for window. Initially, the normal distribution was assessed by the Shapiro-Wilk test. The normal distribution data, representing the homogeneity of the variances, shown by the Levene's test, were then investigated by the one-way analysis of variance (ANOVA) with the Tukey HSD post hoc multiple comparisons. Otherwise, the Dunnett T3 would be applied if the data did not exhibit the homogeneity of the variances. For the data of which the normal distribution was absent but the variance was homogeneous, the Kruskal-Wallis H was applied. To compare the means between 2 data groups, the students' unpaired t-test was used. The significant level was indicated at $p < 0.05$ in any case.

6.4 Results

6.4.1 Microstructure observation

Selected SEM images illustrating microstructure of the as-prepared scaffolds when being viewed on the surface perpendicular to the longitudinal direction are shown in Figure 6.1, while those illustrating the microstructure of the scaffolds when being viewing on the surface perpendicular to the transverse direction are available as Supporting Information (i.e., Figure 6.10). For any given type of the scaffolds, there was no significant difference in the microstructure observed along both directions. On the other hand, marked difference in the microstructure of the scaffolds was observed with increasing the porogen content from 25 to 40% w/w. Specifically, at 25% w/w, a well-defined cubical porous structure, with the polymer mass conforming to the cubic particles of NaCl used in the fabrication process, was evident. Further increasing the porogen content to 30 and 35% w/w was responsible for the ill-defined cubical porous structure observed. At 40% w/w, most of the cubical compartments were substituted with the flake-liked structure. An increase in the porogen content from 25 to 40% w/w should be responsible for the observed increase in the inter-pore connectivity of the scaffolds.

6.4.2 Physical and mechanical characteristics

The as-prepared scaffolds were further characterized for their porosity, pore volume, and pore size (see Table 6.1). Significant increase in the property values was observed for the scaffolds that were prepared with the porogen content ranging between 25 and 35% w/w, while such values for the scaffolds that were prepared with the porogen contents of 35 and 40% w/w were statistically the same. Specifically, the porosity increased from ~94% for the 25xNaCl scaffolds to ~96% for the 35x and the 40xNaCl scaffolds; the pore volume increased from ~12 $cm^3 \cdot g^{-1}$ for the 25xNaCl scaffolds to ~20 $cm^3 \cdot g^{-1}$ for the 35x and the 40xNaCl scaffolds; and, finally, the pore size increased from ~297 μm for the 25xNaCl scaffolds to ~379-408 μm for 35x and 40xNaCl scaffolds. Clearly, the pore size lied in the same range of the porogens used (i.e., 200-400 μm). The increase in the porosity of the scaffolds with increasing the porogen content resulted in an observed

decrease in both the tensile and the compressive properties (see Table 6.2). Specifically, the compressive modulus decreased from ~55 kPa for the 25xNaCl scaffolds to ~35 kPa for the 40xNaCl scaffolds; the compressive strength decreased from ~16 kPa for the 25xNaCl scaffolds to ~12 kPa for the 40xNaCl scaffolds; the tensile modulus decreased from ~719 kPa for the 25xNaCl scaffolds to ~164 kPa for the 40xNaCl scaffolds; and, finally, the tensile strength decreased from ~62 kPa for the 25xNaCl scaffolds to ~20 kPa for the 40xNaCl scaffolds.

6.4.3 Water absorption capability and in vitro degradability

The ability of the as-prepared scaffolds in absorbing water in a basic condition at room temperature within 30 d (720 h) is graphically shown in Figure 6.2. Among the various groups of the scaffolds, the 40xNaCl group exhibited the greatest level of water absorption, while the other three groups showed statistically-similar values. All groups of the scaffolds demonstrated a similar water absorption profile, i.e., an abrupt increase in the level of water absorption during the first 24 h (see Figure 6.11 in Supporting Information) to attain an ultimate value at a long submersion time. Hydrolytic degradation of the scaffolds was evaluated in PBS over a submersion period of 11 weeks. Figure 6.3 shows the remaining weight of the scaffolds after having been submerged in PBS for different time intervals. A slight decrease in the weight of the scaffolds was observed during 5-9 weeks, while an abrupt decrease in their weight was observed during 9-11 weeks. The loss in the weight of these scaffolds at week 11 was an obvious increasing function of the porosity, despite no statistical difference among the four data groups. Morphological changes of the scaffolds after hydrolytic degradation were also studied by SEM (see Figure 6.12 in Supporting Information). Despite the observation of the irregular perforations at some thin parts of the cellular structure, which could be a strong evidence for the hydrolytic decomposition of these scaffolds in the basic medium, the overall porous architecture (i.e., porosity and pore size) of these scaffolds, for the most parts, was retained.

6.4.4 Cytotoxicity and cell/scaffold interaction

Cytotoxicity of the 35xNaCl scaffolds was assessed by observing the relative viability of MC3T3-E1 that were cultured with the extraction media from the scaffolds against that of the cells that were cultured with SFM for 24 h (see Table

6.3). Evidently, the viability of the cells that were cultured with either the extraction media or SFM was statistically the same, a result indicating that the as-prepared PBSu-DCH scaffolds are biocompatible to the bone cells. The non-toxicity of the scaffolds towards the bone cells was also confirmed with lactate dehydrogenase (LDH) cytotoxicity assay (see the additional experiment in Supporting Information). Further preliminary evaluation for the potential use of the scaffolding materials as supports for bone tissue regeneration was carried out by a direct seeding of the bone cells on the surfaces of the scaffolds. Figure 6.4 shows selected SEM images of MC3T3-E1 that had been seeded on the surfaces of the 35xNaCl scaffolds for 24 h. More images are also available (see Figure 6.13 in Supporting Information). Evidently, the cells adhered well on the surface of the scaffolds, with an evidence of cytoplasmic expansion of the cells over the surfaces. Though not shown, further examination of the underlying pores of the scaffolds showed an evidence of MC3T3-E1 that were migratory to the inner-side of the pores.

6.4.5 Inclusion, content, and release of ipriflavone

The existence of ipriflavone in the ipriflavone-loaded PBSu-DCH scaffolds was investigated by FT-IR. Figure 6.5 shows FT-IR spectra of the drug-loaded scaffolds in comparison with those of the pure constituents. In addition to the band characteristic to the ester bonds at 1724 cm^{-1}, the spectra showed the intense bands belonging to the carbonyl groups conjugated with an aromatic compound at 1636 and 1562 cm^{-1} (indicated by the broken arrows) and those of hydroxyl groups at 1260 cm^{-1} (indicated by the solid arrows) (Coates, 2000), which are absent from that of the neat PBSu-DCH scaffolds (viz. the FT-IR spectra of the different types of the neat scaffolds were identical). The amount of ipriflavone that was loaded in the PBSu-DCH scaffolds was reported as either the actual amount of the loaded drug divided by the initial amount of drug loaded (i.e., 10% based on the weight of the polymer; hereafter, the loading efficiency) or the actual amount of the loaded drug divided by the weight of the scaffold specimens (hereafter, the loading capacity) (see Figure 6.6). Evidently, the loading efficiency ranged between 69 and 87%, with a statistical difference being observed between the 25x and the 40xNaCl groups. On the other hand, the loading capacity ranged between 75 and 86%, with no statistical difference among the groups.

The release characteristic of ipriflavone from the drug-loaded PBSu-DCH scaffolds was carried out in a SDS-containing PBS solution at 37°C for a total releasing period of 91 d. The actual amount of the loaded ipriflavone in the scaffolds was used to arrive at the cumulative amount of the drug released from the drug-loaded scaffolds, as shown in Figure 6.7. Interestingly, all of the drugs releasing profiles were identical in their appearance, which could be divided into two phases. Phase 1 correlated to an initial burst release of ipriflavone from the scaffolds within the first 24 h, while phases 2 corresponded to the sustained release of the drug (i.e., day 1 to 60) before the gradual decrease in the rate of the drug release to finally reach a plateau value (i.e., after day 60), respectively. Among the various groups, the cumulative amount of ipriflavone released from the 25xNaCl scaffolds at any given time point was the lowest (with the total amount of the drug released on day 91 being ~55%), while those released from all other groups were statistically the same (with the total amount of the drug released on day 91 being in the range of ~69-71%).

6.5 Discussion

6.5.1 Fabrication technique and scaffold characteristics

The particulate leaching technique has a number of advantages over the freeze-drying technique, based on the physico-chemical properties and cell-culturing benefits of the as-prepared porous scaffolds (Lee *et al.*, 2005). In this technique, the optimal micro-structural morphology, i.e., porosity and pore size, could be readily produced with the choice of an appropriate amount and size of the porogen particles used. Based on the porosity values and the observed inter-pore connectivity of the as-prepared PBSu-DCH scaffolds, the ones that were prepared at the NaCl to PBSu-DCH weight ratio of 30 and 35 showed the most satisfactory microstructure (see Figure 6.1b,c), while those prepared at the NaCl to PBSu-DCH weight ratio of 25 and 40 were unacceptable. Apparently, the microstructure of the scaffolds conformed to the way the NaCl particles accumulated and arranged themselves within the matrix. Large pores with either regular or irregular shape were created by disconnection of the matrix as spaces were occupied by the porogen particles. As presented in Table 6.1, the porosity, the pore volume, and the pore size

significantly increased with an increase in the NaCl contents from 25 to 35% w/w. Between the NaCl contents of 35 and 40% w/w, the difference in the property values of the obtained scaffolds was statistically insignificant. At these contents, the amount of porogens may reach saturation in terms of their packing efficiency.

6.5.2 Physico-mechanical and biological properties

Variation in the microstructure, especially the pore features, of the scaffolds corresponded to their expressive physico-mechanical properties. From the mechanical standpoint, the tensile moduli of the as-prepared porous PBSu-DCH scaffolds (i.e., ~164-719 kPa) were much lower than that of the neat, melt-pressed PBSu films (i.e., ~0.5 GPa) (Li *et al.*, 2005). Comparatively, the variation in the compressive property values among various sample groups was significantly narrower than that in the tensile counterparts (see Table 6.2). Despite the observed decrease in the mechanical property values with increasing the porosity or the pore size of the scaffolds, specific correlations between the property values and the porosity or the pore size could not be made. In addition, the obtained results indicated that the as-prepared scaffold was able to withstand tension over compression. These two deformational modes will be introduced to a scaffold when it is placed in alveolar bone socket and, as an affidavit of its actual applicability; the as-prepared scaffolds were proven to be strong enough as they could be securely placed without any sign of rupture in the narrow captivity of the apical area of a micro-centrifugal tube.

Water absorption capability of a porous scaffold is an indispensable factor determining its actual utilization, as it allows the absorption and retention of blood in the porous structure of the scaffold. Normally, retention of blood leads to thrombosis, which is one of the steps required for bone regeneration. Water absorption capability of the porous scaffold depends significantly on the chemical property of the fabricated material as well as the porosity and the architecture of the porous structure (i.e., pore volume and pore size) (Park *et al.*, 2002). According to the results shown in Table 6.1 and Figures 6.1 and 6.2, the greatest porosity, pore volume, and pore size values and the highest inter-pore connectivity observed for the 40xNaCl scaffolds are the obvious reasons for their greatest water absorption capability. Nevertheless, after 1 h of submersion in PBS, such the property value for

all types of the scaffolds ranged between 88 and 93%, while, after 24 h of submersion, it ranged between 90 and 94%. Obviously, these scaffolds exhibited relatively high water absorption capability.

High water absorption capability is also a condition in favor of hydrolytic degradation of the scaffolds. Here, the hydrolytic degradation of the as-prepared PBSu-DCH scaffolds was studied by evaluating any change in the weight of the materials as a responsive indicator (Shishatskaya *et al.*, 2005). According to the results shown in Figure 6.3, the weights of the 25x, 30x, 35x, and 40xNaCl scaffolds that remained after they had been submerged in PBS for 11 weeks were ~83, ~89, ~92, and ~94% of their initial weights, respectively. As previously noted, the hydrolytic degradation of the scaffolds after submersion in PBS for 11 weeks was also visualized by SEM (see Figure V in Supporting Information), in which decomposition of the materials was observed on the flat surfaces of inter-cellular walls. Despite the evidence of the hydrolytic degradation, physical integrity of the scaffolds was maintained throughout the 11-week period of the investigation. Particularly, there was no sign of significant degradation during the first 2 months. This time period is concomitant with sequential stages during the proliferation and differentiation of bone cells, including proliferation, bone matrix formation and maturation, and mineralization (Wutticharoenmongkol *et al.*, 2007), after which time the scaffolds will finally vanish to provide space for the newly-growing bone tissue (Hutmacher, 2000).

Factually, biodegradation of a polymer is a multi-factorial behavior. Both the degree of crystallinity and the stiffness of the molecular chains were known to be influential in the degradation of PBSu and its co-polymers (Nikolic and Djonlagic, 2001; Nikolic *et al.*, 2003). The theoretical crystallinity of PBSu-DCH, used in this study, was 49.7%. This value was calculated from the ratio of the apparent enthalpy of fusion of this material (i.e., 54.9 $J \cdot g^{-1}$) to the theoretical value for a perfectly crystalline PBSu (i.e., 110.5 $J \cdot g^{-1}$), which was determined based on the group contribution basis (Nikolic and Djonlagic, 2001). Extending PBSu with hexamethylene diisocyanate makes the polymer chains longer and more flexible, which should adversely affect the crystallization of the resulting polymer and, at the same time, increase its degradation susceptibility. Hence, it seems logical to

postulate that the degradation of the as-prepared porous PBSu-DCH scaffolds was enhanced by both the chemical characteristic of the fabricated material and the observed high water absorption capability of the scaffolds.

The legitimacy in the use of the as-prepared porous materials as bone scaffolds was assessed by evaluating their cytotoxicity and ability to support the attachment of MC3T3-E1. The 35xNaCl scaffolds were chosen for such evaluations, due to the balance in their pore architecture, mechanical integrity, and biodegradability. High porosity and large pore sizes encourage *in vivo* bone formation (Lewandrowski *et al.*, 2000; Kuboki *et al.*, 2002; Roy *et al.*, 2003) and the pore sizes greater than ~300 μm were optimal to facilitate vascularization and direct bone formation without preceding cartilage formation (Jin *et al.*, 2000). On the other hand, when the porosity and the pore sizes are too great, the resulting scaffolds may become too weak and degrade too fast, such that their *in vivo* applicability cannot be realized. The 35xNaCl scaffolds were then chosen as a result. Both the indirect and the LDH cytotoxicity evaluations showed that the PBSu-DCH scaffolds were biocompatible to the osteoblast-like cells. Selected SEM images also revealed satisfactory cell/scaffold interaction, as MC3T3-E1 adhered well on the scaffold surfaces. Certain cells showed their flat bodies and broad lamellipodia, indicating that the cell cortex was under tension due to the motility process (Alberts *et al.*, 2002). Since the ability of mammalian cells to attach on a surface influences their capacity to proliferate and differentiate (Anselme, 2000; Sittinger *et al.*, 2004), the as-prepared porous materials could be used as functional bone scaffolds.

6.5.3 Release characteristic of ipriflavone

The potential for use of the as-prepared porous PBSu-DCH materials as effectual drug-releasing porous scaffolds was evaluated using ipriflavone, known for its bone regenerative activity, as the model drug. Both the porosity and the pore size seemed to have little effect on the incorporation of the drug within the scaffolds, as both the loading efficiency and the loading capacity of the drug in the scaffolds were high. Irrespective to the statistical analysis, the 25xNaCl scaffolds exhibited the greatest loading efficiency and the loading capacity on average. This could be a result of the unequal weight of the scaffold specimens used to determine the amount of the as-loaded drug, as the fabrication of the scaffolds was on the iso-volumetric

basis. As a result, the weight of the 25xNaCl scaffold specimens was the greatest, due to the greatest amount of the polymer mass. The highest polymer mass translated to the greatest possibility for drug incorporation, as observed.

The *in vitro* release of ipriflavone from the salt-leached, porous PBSu-DCH scaffolds was complete in ~2 months. The initial burst release of the drug within the first 24 h should be caused by the dissolution of some kinds of drug aggregates that were observed on the superficial cellular surfaces of the scaffolds (results not shown) into the dissolution medium (Perugini *et al.*, 2003). Clearly, the sustained release of the drug in phase 2 (during day 1 to 60) with a constant rate of release (i.e., ~0.64%·d^{-1} for the 25xNaCl scaffolds and ~0.84-0.88%·d^{-1} for the rest of the scaffolds) was the outstanding feature of these scaffolds. Such the time frame unexpectedly matches with the period required for both the proliferation and the differentiation of the bone cells (Hutmacher, 2000; Wutticharoenmongkol *et al.*, 2007) without a noticeable loss in the mass the scaffolds due to degradation (see Figure 3). Interestingly, only the 25xNaCl scaffolds showed the lowest amount of cumulative release of ipriflavone, while all other groups showed an almost identical releasing profile of the drug. This, again, could be due to the fact that the weight of these specimens was the greatest, causing the inter-cellular walls to be thicker than those of the other scaffolds. The thicker inter-cellular walls should greatly influence the diffusion of the drug from the matrix. Nonetheless, other factors, i.e., different loading capacity of the drug within these different scaffolds, could also play a role.

6.6 Conclusion

Poly(1,4-butylene succinate) extended with 1,6-diiocyanatohexane (PBSu-DCH) was successfully fabricated into porous scaffolds by solvent cast and particulate leaching technique, using sodium chloride (NaCl) particles as the leachable component (i.e., porogens). The microstructure of the scaffolds can be tailored by varying the amount of the porogens (i.e., 25, 30, 35, and 40% based on the weight of PBSu-DCH). The porosity, pore volume, pore size, and inter-pore connectivity hypothetically increased, while both the tensile and the compressive strength and modulus hypothetically decreased, with increasing the porogen content.

The suitability of the as-prepared porous materials as bone scaffolds was confirmed by their ability to absorb water quickly even after 1 h after submersion in the phosphate buffer saline solution (PBS; pH 7.4), the negative results on the cytotoxicity evaluation, and their ability to support the attachment of mouse calvaria-derived, pre-osteoblastic cells (MC3T3-E1) that had been seeded on their surfaces for 24 h. The potential for use of the as-prepared porous materials as effectual drug-releasing scaffolds was assessed with ipriflavone as the model drug. Interestingly, the release of ipriflavone from the drug-loaded porous scaffolds was completed in ~2 months, with sustained release of the substance being observed during day 1 to 60). Based on these results, the salt-leached, porous PBSu-DCH scaffolds serve well as alternative biomaterials for bone tissue regeneration, particularly in dental sockets where load-bearing functionality is of prime concern.

6.7 Acknowledgements

The authors acknowledged partial support received from (a) the National Center of Excellence for Petroleum, Petrochemicals, and Advanced Materials (NCE-PPAM), and (b) the Petroleum and Petrochemical College (PPC), Chulalongkorn University.

6.8 References

Alberts, B., Johnson, A., Lewis, J., Raff, M., Roberts, K., and Walter, P. (2002). Molecular biology of the cell (4 ed.). New York: Garland Science.

Altundal, H. and Guvener, O. (2004) The effect of alendronate on resorption of the alveolar bone following tooth extraction. International Journal of Oral and Maxillofacial Surgery, 33(3), 286-293.

Anselme, K. (2000) Osteoblast adhesion on biomaterials. Biomaterials, 21(7), 667-681.

Bodic, F., Hamel, L., Lerouxel, E., Basle, M.F., and Chappard, D. (2005) Bone loss and teeth. Joint Bone Spine, 72(3), 215-221.

Civitelli, R. (1997) In Vitro and In Vivo Effects of Ipriflavone on Bone Formation and Bone Biomechanics. Calcified Tissue International, 61(Suppl 1), S12-S14.

Coates, J. 2000. Interpretation of infrared spectra, A practical approach. In R. A. Meyers (Ed.), Encyclopedia of Analytical Chemistry: 10815-10837. Chichester: John Wiley & Sons Ltd.

Drotleff, S., Lungwitz, U., Breunig, M., Dennis, A., Blunk, T., Tessmar, J., and Gopferich, A. (2004) Biomimetic polymers in pharmaceutical and biomedical sciences. European Journal of Pharmaceutics and Biopharmaceutics, 58(2), 385-407.

Griffith, L.G. (2000) Polymeric Biomaterials. Acta Materialia, 48(1), 263-277.

Hanne, E., Sonis, S., Gallagher, G., and Adwood, D. (1998) Preservation of alveolar ridge with hydroxyapatite-collagen implants in rats. The Journal of Prosthetic Dentistry, 60(6), 729-734.

Hutmacher, D.W. (2000) Scaffolds in tissue engineering bone and cartilage. Biomaterials, 21(24), 2529-2543.

Jahangiri, L., Devlin, H., Ting, K., and Nishimura, I. (1998) Current perspectives in residual ridge remodeling and its clinical implications: A review. J Prosthet Dent, 80(2), 244-237.

Jin, Q.M., Takita, H., Kohgo, T., Atsumi, K., Itoh, H., and Kuboki, Y. (2000) Effects of geometry of hydroxyapatite as a cell substratium in BMP-induced ectopic bone formation. Journal of Biomedical Materials Research, 52(4), 491-499.

Kuboki, Y., Jin, Q., Kikuchi, M., Mamood, J., and Takita, H. (2002) Geometry of artificial ECM: sizes of pores controlling phenotype expression in BMP-induced osteogenesis and chondrogenesis. Connective Tissue Research, 43(2), 529-534.

Lee, S.B., Kim, Y.H., Chong, M.S., Hong, S.H., and Lee, Y.M. (2005) Study of gelatin-containing artificial skin V: fabrication of gelatin scaffolds using a salt-leaching method. Biomaterials, 26(14), 1961-1968.

Lewandrowski, K.U., Gresser, J.D., Bondre, S., Silva, A.E., Wise, D.L., and Trantolo, D.J. (2000) Developing porosity of poly(propylene glycol-co-fumaric acid) bone graft substitutes and the effect on oeteointegration: a preliminary

histology study in rats. Journal of Biomaterials Science, Polymer Edition, 11(8), 879-889.

Li, H., Chang, J., Cao, A., and Wang, J. (2005) In vitro evaluation of biodegradable Poly(butylene succinate) as a novel biomaterial. Macromolecular Bioscience, 5(5), 433-440.

Nikolic, M.S. and Djonlagic, J. (2001) Synthesis and characterization of biodegradble poly(butylenes succinate-co-butylene adipate)s. Polymer Degradation and Stability, 74(2), 263-270.

Nikolic, M.S., Poleti, D., and Djonlagic, J. (2003) Synthesis and characterization of biodegradble poly(butylenes succinate-co-butylene fumarate)s. European Polymer Journal, 39(11), 2183-2192.

Park, S.-N., Park, J.-C., Kim, H.O., Song, M.J., and Suh, H. (2002) Characterization of porous collagen/hyaluronic acid scaffold modified by 1-ethyl-3-(3-dimethylaminopropyl)carbodiimide cross-linking. Biomaterials, 23(4), 1205-1212.

Perugini, P., Genta, I., Conti, B., Modena, T., Cocchi, D., Zaffe, D., and Pavanetto, F. (2003) PLGA microspheres for oral osteopenia treatment: preliminary "invitro"/ "in vivo" evaluation. International Journal of Pharmaceutics, 256(1), 153-160.

Roy, T.D., Simon, J.L., Ricci, J.L., Rekow, E.D., Thompson, V.P., and Parsons, J.R. (2003) Performance of degradable composite bone repair products made via three-dimensional fabrication techniques. Journal of Biomedical Materials Research Part A, 66A(2), 281-291.

Shishatskaya, E.I., Volvova, T.G., Gordeev, S.A., and Puzyr, A.P. (2005) Degradation of P(3HB) and P(3HB-co-3HV) in biological media. Journal of Biomaterials Science, Polymer Edition, 16(5), 643-657.

Sittinger, M., Hutmacher, D.W., and Risbud, M.V. (2004) Current strategies for cell delivery in cartilage and bone regeneration. Current opinion in biotechnology. Current Opinion in Biotechnology, 15(5), 411-418.

Wiesen, M. and Krrzis, R. (1998) Preservation of the alveolar ridge at implant sides. Periodontal Clinical Investigations, 20(2), 17-20.

Wiesmann, H.P., Joos, U., and Meyer, U. (2004) Biological and biophysical principles in extracorporal bone tissue engineering Part II. International Journal of Oral and Maxillofacial Surgery, 33(6), 523-530.

Wutticharoenmongkol, P., Pavasant, P., and Supaphol, P. (2007) Osteoblastic Phenotype Expression of MC3T3-E1 Cultured on Electrospun Polycaprolactone Fiber Mats Filled with Hydroxyapatite Nanoparticles. Biomacromolecules, 8(8), 2602-2610.

Yaffe, A., Binderman, I., Breuer, E., Pinto, T., and Golomb, G. (1999) Disposition of alendronate folllowing local delivery in a rat jaw. Journal of Periodontology, 70(8), 893-895.

Table 6.1 Porosity, pore volume, and pore size of the as-prepared PBSu-DCH scaffolds

Sample	Porosity* (%)	Pore volume** ($cm^3 \cdot g^{-1}$)	Pore size** (μm)
25xNaCl	93.96 ± 0.24^a	11.97 ± 0.51^a	296.7 ± 47.0^a
30xNaCl	94.75 ± 0.24^b	13.91 ± 0.67^b	331.7 ± 66.1^b
35xNaCl	96.20 ± 0.31^c	19.58 ± 1.66^c	378.9 ± 55.8^c
40xNaCl	96.27 ± 0.14^c	19.90 ± 0.74^c	407.8 ± 69.5^c

^{a,b,c} are significantly different at $p < 0.05$ for an individual feature; *one way ANOVA with Tukey HSD, **One way ANOVA with Dunnett T3; $n = 5$ for porosity and pore volume, $n = 50$ for pore size

Table 6.2 Mechanical properties of the as-prepared PBSu-DCH scaffolds

Sample	Compessive modulus* (kPa)	Compressive strength* (kPa)	Tensile modulus* (kPa)	Tensile strength** (kPa)
25xNaCl	54.75 ± 4.87^{a}	15.66 ± 1.15^{a}	719.4 ± 28.4^{a}	61.63 ± 3.67^{a}
30xNaCl	$52.90 \pm 2.70^{a,b}$	15.24 ± 0.75^{a}	301.7 ± 40.2^{b}	38.27 ± 3.44^{b}
35xNaCl	47.17 ± 2.34^{b}	13.30 ± 0.71^{b}	240.5 ± 20.1^{c}	36.51 ± 1.98^{b}
40xNaCl	35.17 ± 4.26^{c}	11.94 ± 1.13^{b}	163.6 ± 36.9^{d}	20.17 ± 1.62^{c}

*At 20% strain, **At rupture; ^{a,b,c,d} are significantly different at $p < 0.05$ for an individual feature; One way ANOVA with Tukey HSD

Table 6.3 Indirect cytotoxicity evaluation of the as-prepared 35xNaCl scaffolds using mouse calvaria-derived, pre-osteoblastic cells (MC3T3-E1)

Sample No.	Absorbance @ 540 nm	
	Control group	Experimental group
1	0.094	0.118
2	0.123	0.138
3	0.147	0.116
4	0.114	0.110
Average	0.119 ± 0.022*	0.120 ± 0.012*

*$p < 0.05$ significant level; Student's unpaired t-test

ADDITIONAL EXPERIMENT
LACTATE DEHYDROGENASE (LDH) CYTOTOXICITY ASSAY

Experimental detail

In addition to the MTT assay, toxicity of the 35xNaCl scaffolds towards mouse calvaria-derived, pre-osteoblastic cells (MC3T3-E1) was also assessed with the LCH cytotoxicity assay (Cayman's LDH Cytotoxicity Assay Kit, Cayman Chemical, USA). Briefly, MC3T3-E1 were cultured in minimum essential medium (MEM; Sigma-Aldrich, USA), supplemented by 10% fetal bovine serum (FBS; Biochrom, Germany), 1% L-glutamine (Invitrogen, USA) and a 1% antibiotic and antimycotic formulation (containing penicillin G sodium, streptomycin sulfate, and amphopericin B (Invitrogen Corp.)) in wells of a 24-well culture plate at 3×10^4 cells/well. Simultaneously, a scaffold specimen was submerged in the same culture medium and both the cells and the scaffold specimen were incubated at 37°C in a humidified atmosphere containing 5% CO_2 for 24 h. The scaffold specimen was then removed and placed on top of the cultured cells and both the cells and the scaffold specimen were incubated further for another 24 h. After the required time, the scaffold specimen was removed and the culture medium was transferred to an Eppendrof tube. After centrifugation at 2000 rpm for 5 m, 200 μL of the supernatant was then transferred to wells of a 24-well culture plate and 200 μL of the reaction mixture was added. Finally, after 30 min of rotary agitation at room temperature, the absorbance of the sample solution at 490 nm was measured using a Thermospectronic Genesis10 UV/Visible spectrophotometer. The experiment was carried out in quadruplicate.

Results

The absorbance values form the LDH cytotoxicity test are shown in the following table:

Table 6.4 Indirect cytotoxicity evaluation of the as-prepared 35xNaCl scaffolds using mouse calvaria-derived, pre-osteoblastic cells (MC3T3-E1) assessed with the LCH cytotoxicity assay

Sample No.	Absorbance @ 490 nm	
	Control group	Experimental group
1	0.604	0.458
2	0.599	0.544
3	0.556	0.482
4	0.583	0.584
Average	0.586 ± 0.022*	0.517 ± 0.058*

* $p < 0.05$ significant level; Student's unpaired t-test

Apparently, the average absorbance value of the experimental group was insignificantly lower than that of the control group. This indicates that the amount of LDH released from the MC3T3-E1 upon exposure to the PBS-DCH scaffolds was not different from the non-exposure ones. The obtained result confirms that the tested scaffolds were non-toxic to the bone cells.

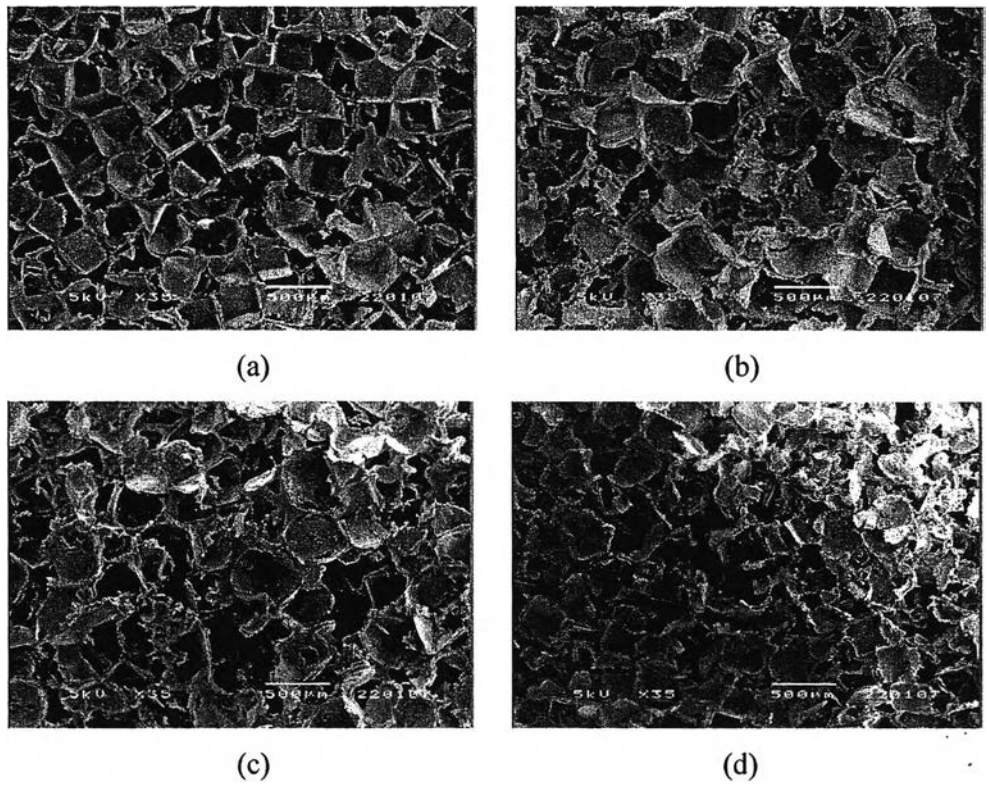

Figure 6.1 Selected SEM images illustrating microstructure of the as-prepared PBSu-DCH scaffolds, i.e., (a) 25x, (b) 30x, (c) 35x, and (d) 40xNaCl scaffolds, when being viewed on the surface perpendicular to the longitudinal direction (i.e., cross sections).

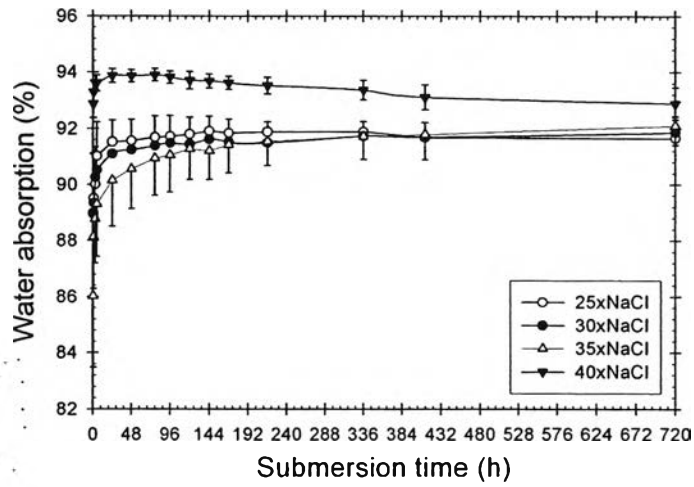

Figure 6.2 Water absorption capability of the as-prepared PBSu-DCH scaffolds that had been submerged in 10 mM PBS at room temperature as a function of submersion time.

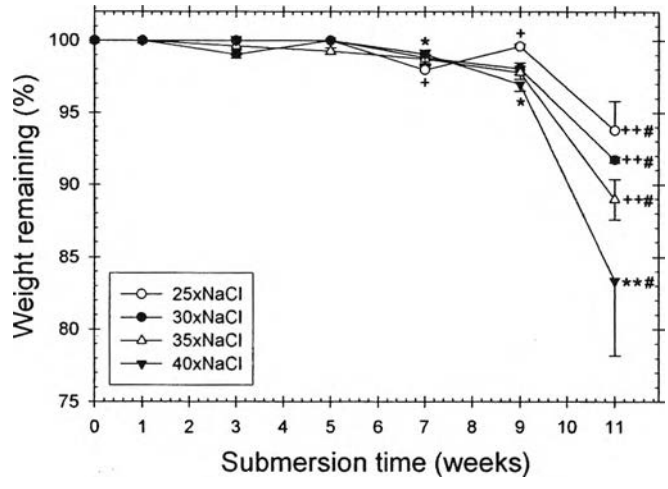

Figure 6.3 Weight of the as-prepared PBSu-DCH scaffolds that remained after submersion in 10 mM PBS for various submersion times. *$p < 0.05$, ++$p < 0.05$; One-way ANOVA with Dunnett T3. #$p < 0.05$; Kruskal-Wallis H test.

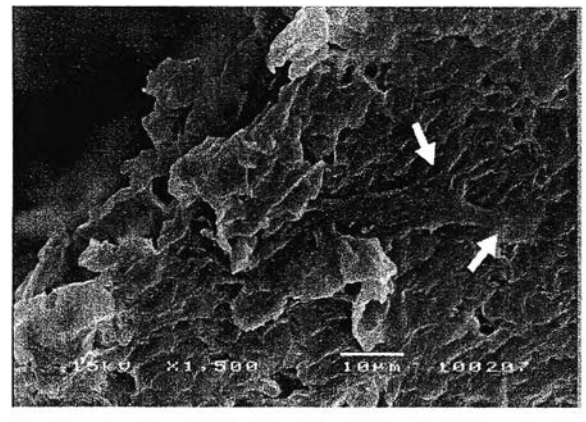

(a)

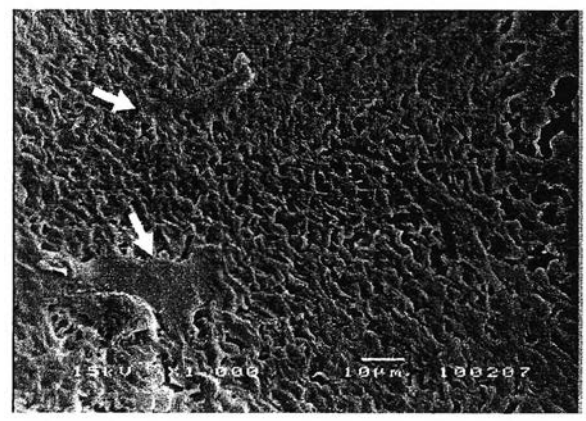

(b)

Figure 6.4 Selected SEM images illustrating morphology of MC3T3-E1 that were seeded on the surface of the 35xNaCl scaffolds for 24 h. White arrows show the cytoplasmic edge of the cells.

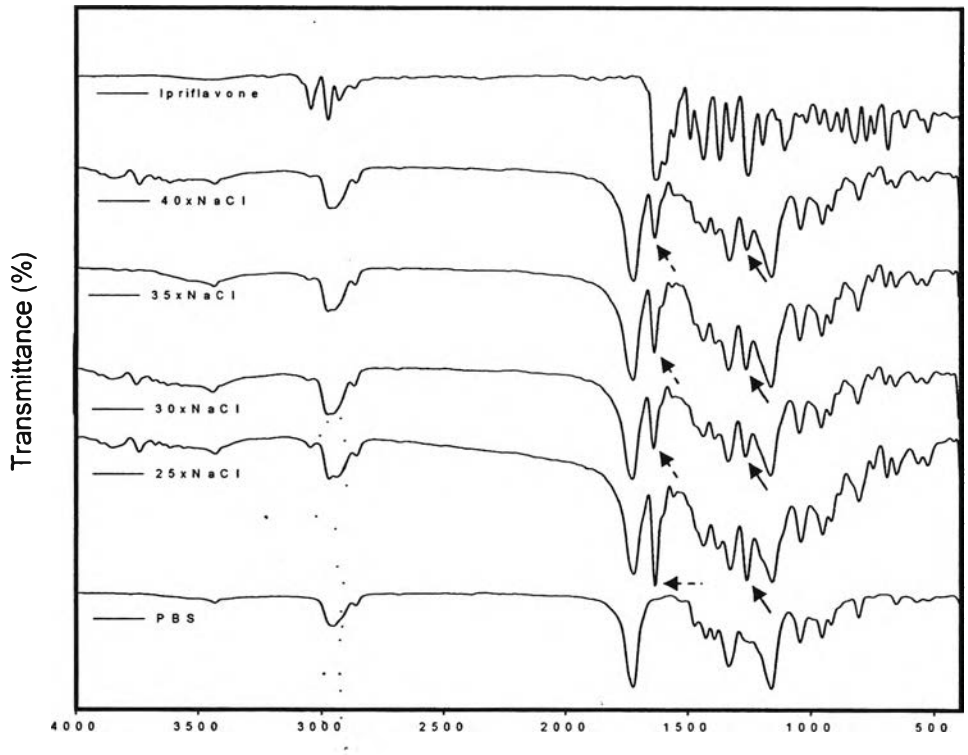
Ipriflavone
40xNaCl
35xNaCl
30xNaCl
25xNaCl
PBS
Transmittance (%)
4000
3500
3000
2500
2000
1500
1000
500

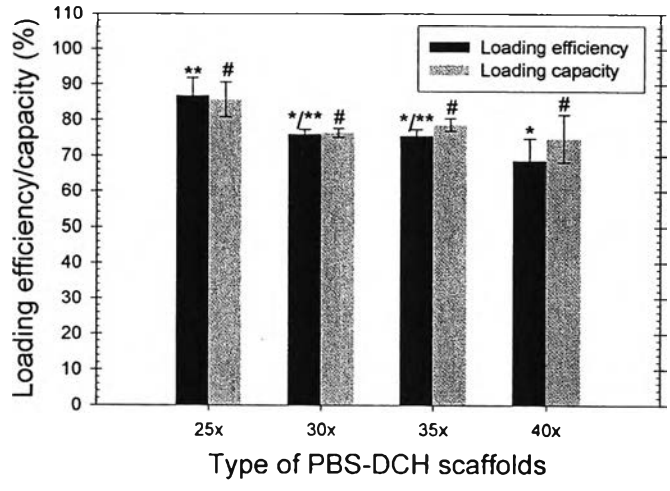

Figure 6.6 Loading efficiency/capacity of ipriflavone in the ipriflavone-loaded PBSu-DCH scaffolds. *$p < 0.05$, #$p < 0.05$; Kruskal-Wallis H test.

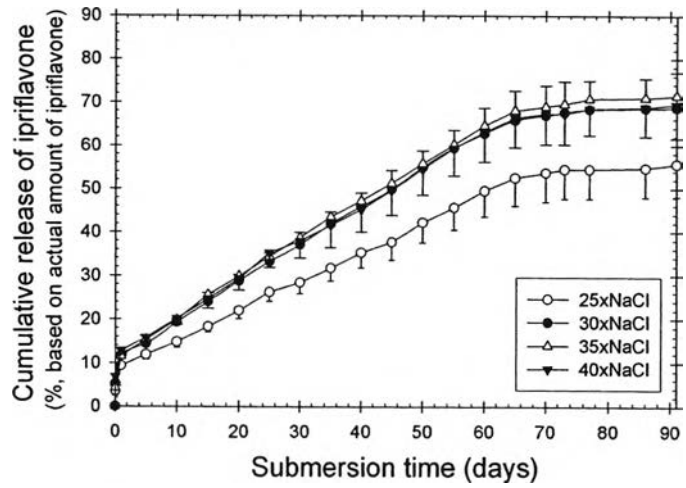

Figure 6.7 Cumulative releasing profiles of ipriflavone from the ipriflavone-loaded PBSu-DCH scaffolds in a SDS-containing PBS solution at 37°C.

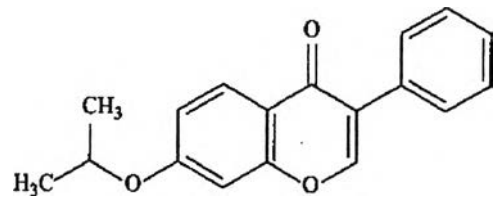

Figure 6.8 Chemical structure of ipriflavone.

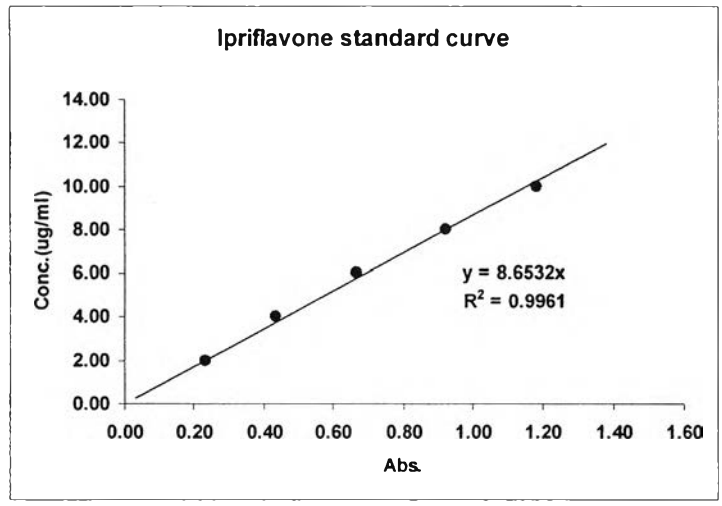

Figure 6.9 Calibration curve illustrating a linear relationship between the ipriflavone solution concentration and the UV absorbance at 249 nm.

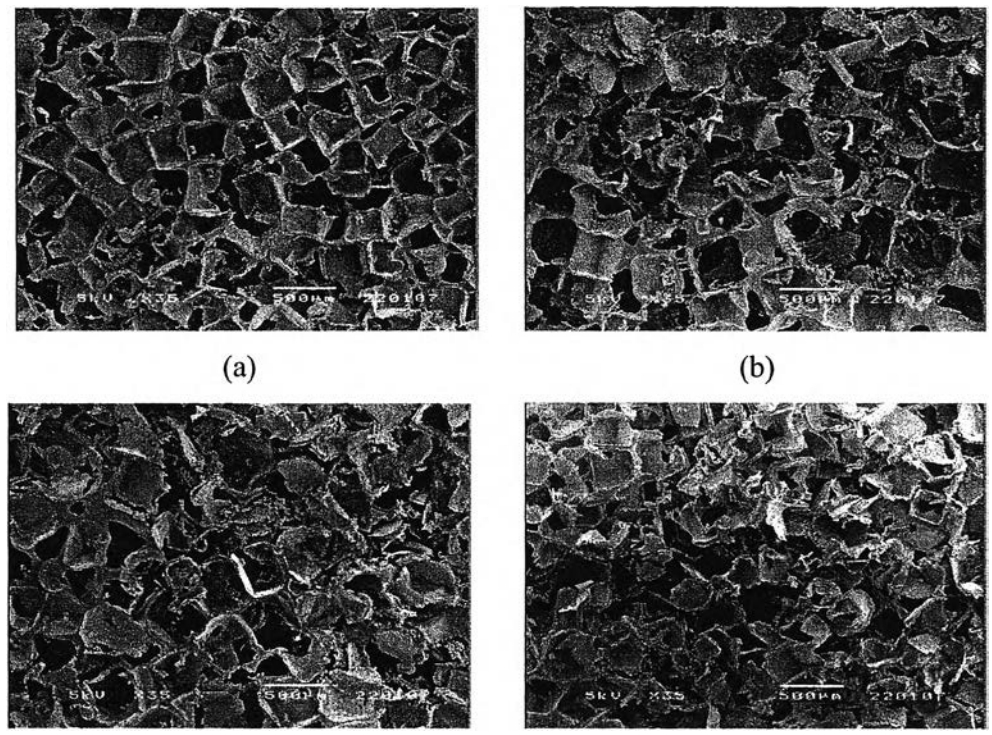

Figure 6.10 Selected SEM images illustrating microstructure of the as-prepared PBS-DCH scaffolds, i.e., (a) 25x, (b) 30x, (c) 35x, and (d) 40xNaCl scaffolds, when being viewed on the surface perpendicular to the transverse direction (i.e., longitudinal sections).

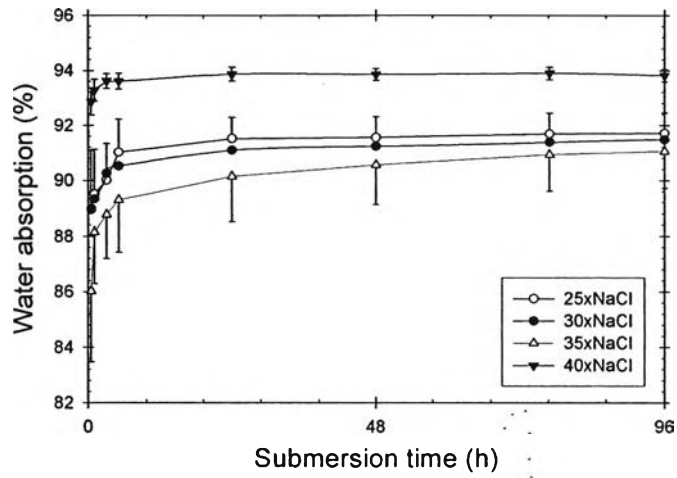

Figure 6.11 Water absorption capability of the as-prepared PBS-DCH scaffolds that had been submerged in 10 mM phosphate buffer saline solution (PBS) at room temperature as a function of submersion time (shown during the first 96 h).

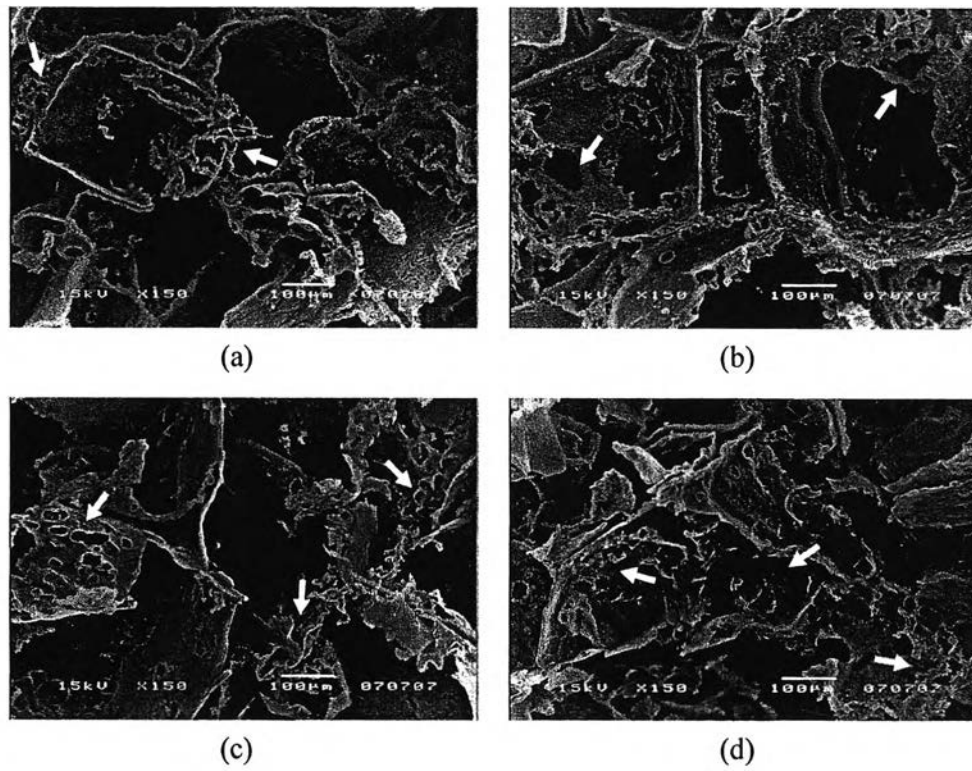

Figure 6.12 Change in the morphology of the as-prepared PBS-DCH scaffolds after submersion in 10 mM PBS at 37°C for 11 weeks.

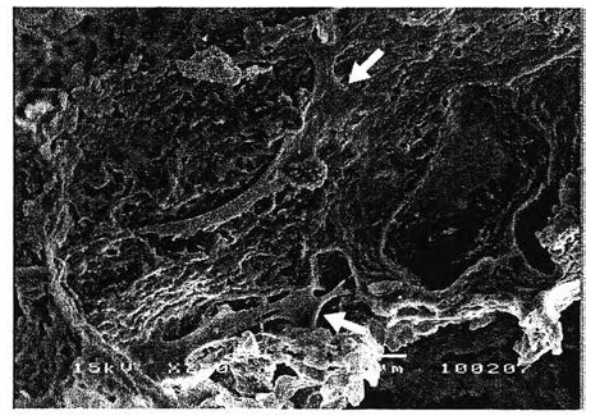

(a)

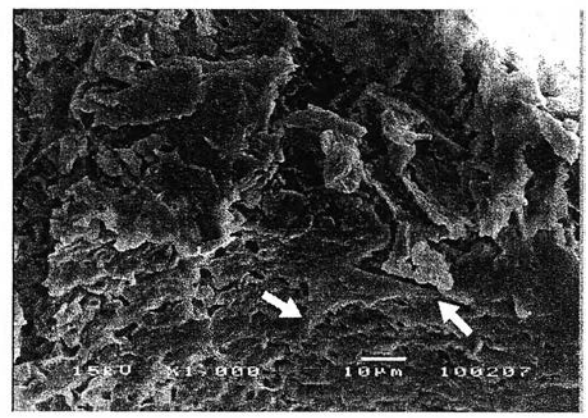

(b)

Figure 6.13 Selected SEM images illustrating morphology of MC3T3-E1 that were seeded on the surface of the 35xNaCl scaffolds for 24 h. White arrows show the cytoplasmic edge of the cells.